Inhomogeneous interlayer Josephson coupling in $\kappa-(\mathrm{BEDT-TTF})_2\mathrm{Cu}(NCS)_2$

1999 J. Phys.: Condens. Matter 11 2007

(http://iopscience.iop.org/0953-8984/11/8/013)

J. Phys.: Condens. Matter **11** (1999) 2007–2016. Printed in the UK PII: S0953-8984(99)99496-1

Inhomogeneous interlayer Josephson coupling in κ-(BEDT-TTF)$_2$Cu(NCS)$_2$

J R Kirtley†, K A Moler‡‖, J A Schlueter§ and J M Williams§

† IBM Research, PO Box 218, Yorktown Heights, NY 10598, USA
‡ Department of Physics, Princeton University, Princeton, NJ 08544, USA
§ Chemistry and Material Science Division, Argonne National Laboratory, Argonne, IL 60439, USA

Received 20 November 1998

Abstract. In a layered superconductor, the interlayer coupling strength determines the spatial variation of the magnetic fields parallel to the layers. Scanning SQUID microscope images of an edge of a single crystal of the layered organic superconductor κ-(BEDT-TTF)$_2$Cu(NCS)$_2$ show regions of inhomogeneous coupling as well as trapped interlayer Josephson vortices. Quantitative modelling of individual isolated vortices indicates an interlayer penetration depth $\lambda_\perp \sim 60$ μm. Previous bulk measurements that indicated a weaker interlayer coupling may have been dominated by inhomogeneities.

1. Introduction

Many unconventional superconductors, notably cuprates and some organics, have a strongly anisotropic layered structure. The layered superconductors are commonly modelled as a stack of 'conventional' superconducting layers with Josephson coupling between the layers: the Lawrence–Doniach model [1]. The interlayer coupling strength can be characterized by the interlayer penetration depth, $\lambda_\perp$, which is related to the interlayer critical current density J_0 by [2]

$$\lambda_\perp = (c\phi_0/8\pi^2 s J_0)^{1/2} \tag{1}$$

where c is the speed of light, $\phi_0 = hc/2e$ is the superconducting flux quantum, h is Planck's constant, e is the charge on the electron, and s is the interlayer spacing. In the context of the Lawrence–Doniach model, Clem and Coffey derived expressions for the structure of vortices parallel to the layers (figure 1(a)), called 'interlayer Josephson vortices' [2]. Except at the smallest length scales, these vortices are identical to vortices in an anisotropic London model. The strength of the interlayer coupling is an important parameter in any phenomenological description of these materials, but it can be difficult to make reliable measurements of penetration depths.

In this paper, we report the direct observation of interlayer vortices parallel to the planes of the organic superconductor κ-(BEDT-TTF)$_2$Cu(NCS)$_2$ ($T_c = 9.0$ K), and use theoretical expressions for the shape of an interlayer vortex at the surface [3] to find the interlayer or a-axis penetration depth $\lambda_\perp \sim 60$ μm. In a superconductor with uniform coupling, the only magnetic features would be identical vortices and Meissner screening currents that penetrate

‖ Permanent address: Department of Applied Physics, Stanford University, Stanford, CA 94305, USA.

0953-8984/99/082007+10$19.50

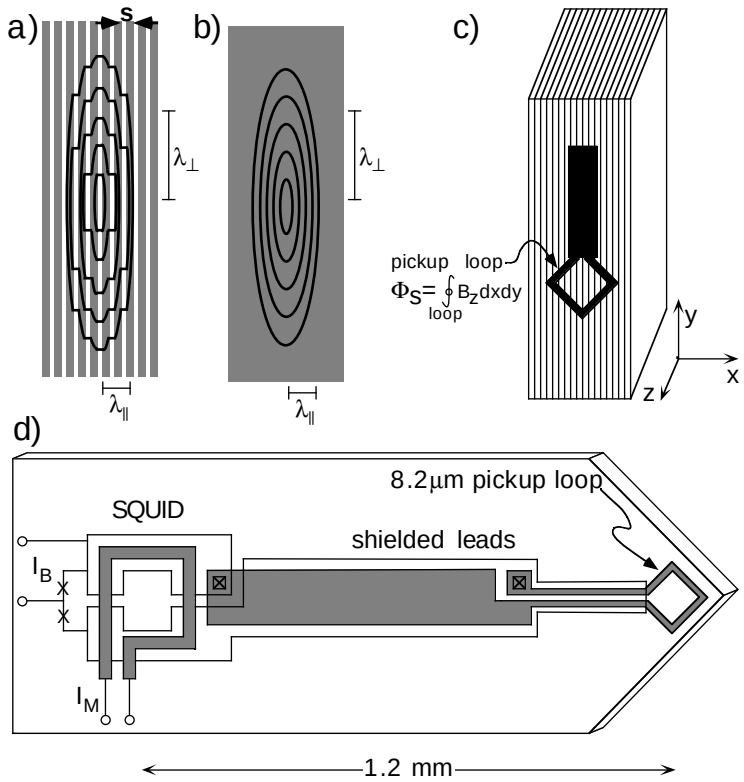

Figure 1. (a) A sketch of the current flow, equivalent to contours of constant magnetic field, for an isolated interlayer Josephson vortex with its axis along z. The grey regions indicate superconducting layers with Josephson coupling between the layers. The interlayer spacing s, in-plane penetration depth $\lambda_\parallel$, and interlayer penetration depth $\lambda_\perp$ are shown. (b) For length scales large compared to s, the vortex structure becomes indistinguishable from a vortex in a continuous anisotropic London model. (c) A sketch of the measurement geometry showing the pickup loop parallel to the conducting b–c planes of a single crystal of κ-(BEDT-TTF)$_2$Cu(NCS)$_2$ (not drawn to scale). (d) A schematic diagram of the SQUID sensor. The signal is proportional to changes in the amount of magnetic flux through the pickup loop.

on the length scale of the penetration depth. In contrast, we observe magnetic flux penetration on a distribution of length scales up to many times $\lambda_\perp$, indicating an inhomogeneous interlayer coupling.

The value $\lambda_\perp \sim 60\ \mu$m is also of interest as a test for a candidate mechanism for superconductivity in these materials. It has been proposed that non-Fermi-liquid behaviour in the normal state may drive the material superconducting because of a change in the interlayer coupling between the two states [4–7]. This class of mechanisms is known as the interlayer tunnelling (ILT) model [8]. In the simplest version of the ILT model, the condensation energy, E_c is supplied entirely by a change in the c-axis kinetic energy. As has been pointed out by Leggett [8], by Anderson [7], and by Chakravarty *et al* [6], the model therefore requires an exact quantitative relationship between the interlayer penetration depth and the condensation energy:

$$\lambda_{ILT} = \left(\frac{mc^2}{E_c} \frac{a_0 A}{4\pi s} \right)^{1/2} \tag{2}$$

where $E_c = H_c^2 As/8\pi$ is the condensation energy per formula unit, H_c is the thermodynamic critical field, A is the area per formula unit, m is the mass of the electron, and a_0 is the Bohr magneton. Using $H_c(0) = 500$ G [9] and $s = 15.24$ Å, the theoretical penetration depth for the ILT model is about ten microns. The interlayer coupling in κ-(BEDT-TTF)$_2$Cu(NCS)$_2$ therefore appears to be too weak to support the current published versions of the ILT model.

Coherent Josephson pair transport in this material has previously been demonstrated [10], confirming the applicability of the Lawrence–Doniach model, but without providing a direct value for the coupling. Recently, through a direct observation of the Josephson plasma resonance, Shibauchi *et al* inferred a penetration depth of $\lambda_\perp = 120$ μm [11]. For other materials, we have observed reasonable agreement between the plasma resonance and the penetration depth [12]. However, we note that deriving the penetration depth from the plasma resonance requires the dielectric constant of the interlayer medium, which can be difficult to obtain. Several measurements of the in-plane penetration depth in this material have been made [13]. The interlayer penetration depth has previously been reported to be $\lambda_\perp \sim 1$ mm [14–16] and $\lambda_\perp \sim 200$ μm [9] from measurements of the bulk magnetic susceptibility, and 30 μm from measurements of the surface impedance [17]. The authors of reference [9] speculated that the discrepancy between these two values may have resulted from cracks or other inhomogeneities, and pointed out that values for $\lambda_\perp$ obtained from bulk susceptibility should be considered as upper limits. Indeed, our observation of inhomogeneous coupling, even in high-quality crystals, seems to confirm this speculation. The inhomogeneous background presents difficulties in the analysis of our local-probe data, and could be expected to dominate bulk susceptibility measurements.

2. Technique

The measurements were made with a scanning SQUID microscope [18], in which a sample is scanned relative to a superconducting pickup loop oriented approximately parallel to the sample surface (figure 1(c)). At any given position, the magnetic flux through the pickup loop, Φ_s, is the integral of the z-component of the magnetic field over the area of the pickup loop. The data are represented as intensity maps of Φ_s versus the position of the pickup loop in the x–y plane. The pickup loop is fabricated with well-shielded leads to an integrated niobium SQUID (figure 1(d)). For these measurements, we used a diamond-shaped pickup loop with sides of length $L = 8.2$ μm and 0.8 μm linewidth. The silicon substrate upon which the SQUID is fabricated only extends a few microns from the edge of the pickup loop. The height of the loop above the sample is given by

$$z_0 = l \sin\theta + a$$

where $\theta \sim 20^\circ$ is the angle between the substrate and sample, $l \sim 8$ μm is the spacing between the loop centre and the tip contact point, and $a \sim 2$ μm is the thickness of a protective layer of nail varnish on the tip. Modelling of Abrikosov vortices in cuprate superconductors using the present tip alignment and coating procedures yielded effective loop heights of $z_0 \sim 5$ μm. Both the sample and the SQUID were immersed in liquid helium at 4.2 K in a magnetically shielded cryostat with a residual magnetic field of several milligauss and an uncontrolled orientation. The residual magnetic field B_z along the z-direction, perpendicular to the measurement plane, was determined by imaging and counting trapped vortices in a niobium film adjacent to the sample. A small magnet was used to adjust B_z. The data presented here were taken with the external field set to zero before cooling the sample through the transition temperature, to achieve a nominally zero-field-cooled state.

3. Samples

The single-crystal κ-(BEDT-TTF)$_2$Cu(NCS)$_2$ samples used in this study were prepared by a standard electrochemical crystal growth procedure. The electrolyte solution consisted of 18-crown-6, CuSCN, and KSCN dissolved in 90% 1, 1, 2-trichloroethane/10% ethanol. BEDT-TTF was dissolved in the anode solution. The crystals were grown on platinum electrodes with an applied current density of 0.2 μA cm^{-2} [20]. We studied three different samples. All of the images shown in this paper were taken for the same single crystal, which had a mid-point critical temperature of $T_c = 9.0$ K, and a transition width (10%–90%) of 0.4 K.

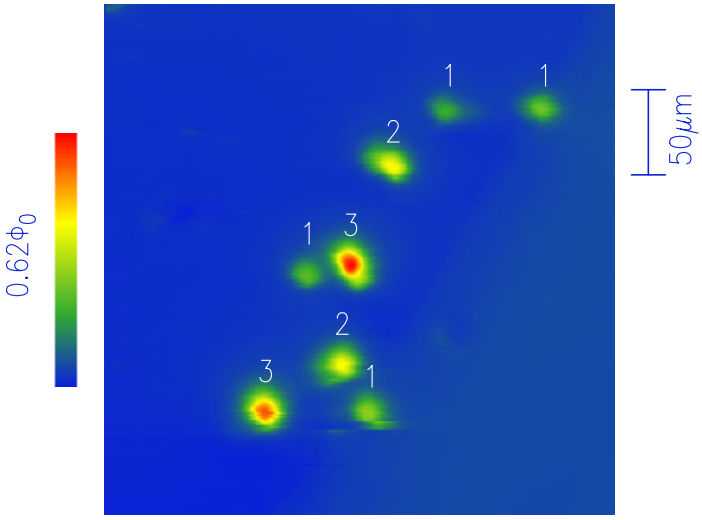

Figure 2. An image of a 300 × 300 μm^2 area of the crystal face, cooled in nominal zero field and imaged at 4.2 K, with the measurement plane parallel to the conducting *b*–*c* planes. This image contains seven vortex-trapping sites, with the number of vortices per site as labelled in the figure.

4. Results

The crystals were mounted so as to image either the surface parallel to the conducting layers (figure 2), which we call the crystal face, or the surface along the edges of the conducting layers (figure 3), which we call the crystal edge. After cooling the sample in a field of a few milligauss, the images of the crystal face showed several trapped vortices (figure 2) against a clean zero-field background. Each of the bright spots in figure 2 contains approximately one, two, or three integral flux quanta as labelled in the figure. These assignments were made by modelling [18] the vortex bundles as magnetic monopole sources with varying total flux. It is difficult to precisely determine the total amount of flux in each because of their irregular shapes. The locations of the vortices are presumably determined by a disorder-induced pinning potential, which in this case must be strong enough to overcome the vortex–vortex repulsive force. With an 8 μm pickup loop, we are unable to resolve the location of the vortices with sufficient accuracy to say whether they are isolated on the scale of the in-plane penetration depth. In our experience, almost all type-II superconductors show isolated trapped vortices when cooled in nonzero field. In niobium and cuprate superconductors these vortices are well pinned and are not observed to move below 4 K. The vortices shown in figure 2 did

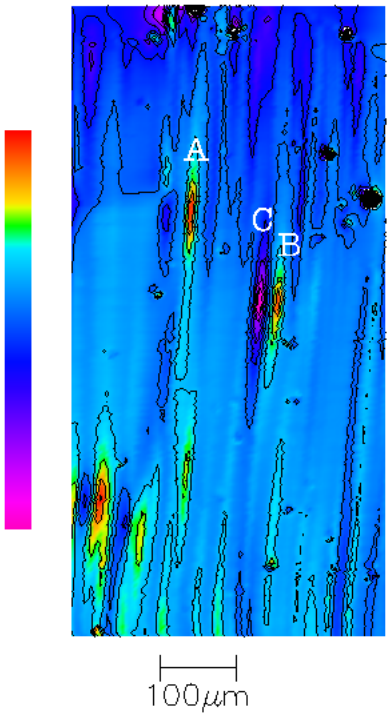

Figure 3. A scanning SQUID microscope image of a 400 × 800 μm^2 area of the crystal edge. The crystal was cooled in nominally zero field and imaged at 4.2 K. Three interlayer vortices are labelled, two with fields directed out of the surface (A, B), and one with fields directed into the surface (C). The colour table used in this image corresponds to a full-scale variation of $0.05\Phi_0$ threading through the pickup loop.

move, however. Scans repeated every hour or so showed three vortices in new locations over the course of a few days. This observation is qualitatively consistent with the weak pinning potential in these materials [9].

The images of the crystal edge, which are the main focus of this paper, were markedly different. When cooled in fields of a few milligauss or more, the crystal edge showed disordered patterns of magnetic flux with a distribution of characteristic length scales each of the order of a hundred microns. Even when the crystals were cooled in nominally zero field, an inhomogeneous background remained, as shown in figure 3. Positive flux penetrates in vertical stripes from the bottom of the image, and negative flux penetrates from the top. There is noticeable rippling of the fields parallel to the layered planes throughout the crystal, as can be seen from the contour lines placed on the image. We speculate that these rippling features result from penetration of the external field on a length scale which is longer than the intrinsic interlayer penetration depth, and that these regions with weak coupling result from mechanical or chemical defects.

In regions of the crystal with relatively homogeneous backgrounds, the predominant magnetic features are elliptically shaped concentrations of magnetic flux, with both positive and negative signs. In four separate coolings, we observed nine such objects in different parts of the crystal, always with the same distinctive shape and size. Accordingly we tentatively identified these objects as the intrinsic interlayer Josephson vortices, despite the inhomogeneous background. It is difficult to precisely determine the amount of flux carried by

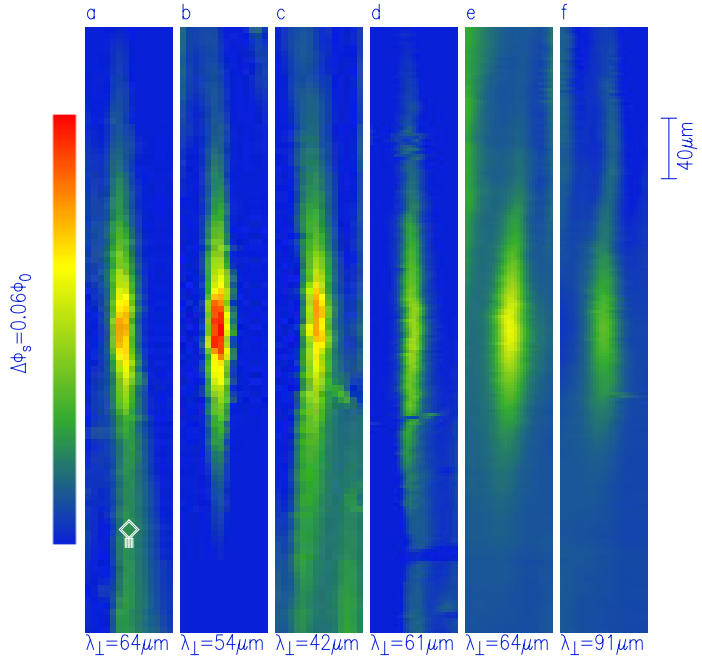

Figure 4. Images of six interlayer vortices for three different coolings. Longitudinal cross-sections vertically through the centres of the images are used for the fits shown in figure 5. A scaled schematic drawing of the SQUID pickup loop used for these measurements is shown as an overlay in panel (a).

each vortex because they extend over large distances with a locally varying background field, but each includes approximately a single flux quantum.

Figure 4 shows a close-up of six interlayer vortices. The extent of each vortex perpendicular to the layers (along x) is limited by the spatial resolution of the pickup loop. In contrast, the vortex extends a distance in y which is large compared to the size of the pickup loop. Taking into account the effect of the surface on the fields, and assuming that the relatively large size of the pickup loop effectively integrates the magnetic field of the vortex over x, we can estimate the penetration depth from the size of the vortices in the image. With these assumptions, the theoretical full width at half-maximum of the vortex image is $1.8\,\lambda_\perp$ [3]. This simple estimate gives an interlayer penetration depth of $\lambda_\perp = 61 \pm 6\ \mu$m for the vortices that we observed. Kogan and co-workers have derived expressions for the magnetic structure of an anisotropic vortex at a superconductor–vacuum interface in an anisotropic London model [3]. We use these expressions for quantitative modelling of the observed vortex shape. Outside the superconductor, the z-component of the magnetic field of an isolated interlayer vortex is given by [3]

$$h_z(\boldsymbol{r}, z) = -\int \frac{\mathrm{d}^2\boldsymbol{k}}{(2\pi)^2}\, k\phi(\boldsymbol{k})\mathrm{e}^{\mathrm{i}\boldsymbol{k}\cdot\boldsymbol{r}-kz} \tag{3}$$

where

$$\phi(\boldsymbol{k}) = -\frac{\phi_0(1 + m_1k_x^2)}{m_3\alpha_3[m_1k_x^2\alpha_3(k + \alpha_1) + k\alpha_3 + k_y^2]}. \tag{4}$$

Here, $\alpha_1 = ((1 + m_1k^2)/m_1)^{1/2}$, $\alpha_3 = ((1 + m_1k_x^2 + m_3k_y^2)/m_3)^{1/2}$, $k = (k_x^2 + k_y^2)^{1/2}$, $m_1 = \lambda_\parallel^2/\lambda^2$, $m_3 = \lambda_\perp^2/\lambda^2$, $\lambda = (\lambda_\parallel^2\lambda_\perp)^{1/3}$, $\lambda_\parallel$ is the in-plane penetration depth, x is

the distance perpendicular to the planes, and y is the distance parallel to the planes. The Fourier transform is obtained numerically, and the resulting magnetic field is summed over the geometry of the pickup loop to find the flux threading the loop as the SQUID scans. Assuming that $\lambda_{\parallel} = 0.5\ \mu$m [19], and accounting for the locally varying background in these images, fits may be made with three free parameters: the background signal F_B, the height of the pickup loop z_0, and the interlayer penetration depth $\lambda_{\perp}$. The magnetic amplitude of the vortex image is determined by the height of the pickup loop, assuming that the vortex contains one flux quantum. $\lambda_{\perp}$ is the only parameter which plays a significant role in determining the length of the vortices. Thus, our free parameters are not strongly correlated and each may be well determined in a fit.

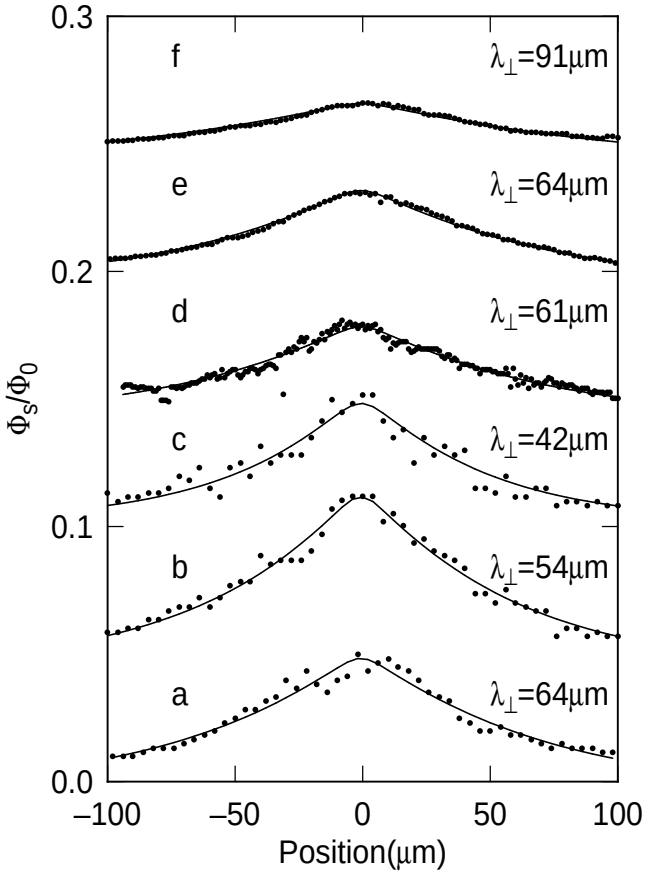

Figure 5. Cross-sections through the vortices in figure 4, offset by $0.05\phi_0$ for clarity. The solid lines are fits as described in the text. The best-fit values for z_0 are 0.9 μm (a), 0.54 μm (b), 3.1 μm (c), 2.7 μm (d), 2.3 μm (e), and 2.8 μm (f).

Figure 5 shows fits to cross-sections through the vortices in figure 4, using the background, z_0, and $\lambda_{\perp}$ as nonlinear free parameters. This procedure leads to different values for z_0 for the vortices, although during a given run this height should be a constant set by the experimental geometry. We attribute this error to inhomogeneities in the magnetic properties in these samples. Within this limitation, these fits show that the Kogan–Clem model provides a reasonable description of the shape of the vortices. The interlayer penetration depth varies

by a factor of two for the six vortices, resulting in the value $\lambda_\perp = 63 \pm 15$ μm. The quoted uncertainty in this value is only statistical and does not include the systematic uncertainty resulting from the inhomogeneous background. We have previously discussed additional systematic errors associated with an uncertainty in the effective shape of the SQUID pickup loop [3]. In this case, we expect these errors to be small, since the interlayer penetration depth is much larger than the size of the pickup loop.

This measured length can be compared with other measurements. In comparison with the values obtained from the magnetic susceptibility for this material, 1 mm [16] and 200 μm [9], our observations confirm that the bulk susceptibility technique is sensitive to inhomogeneities, and indicate the usefulness of local probes for studying potentially inhomogeneous materials. There is also a discrepancy between our value, $\lambda_\perp \sim 60$ μm, and the value determined from the Josephson plasma resonance, $\lambda_\perp = 120$ μm [11]. One possible explanation is that the samples come from different sources. We also note that determining the penetration depth from the plasma frequency requires knowing the dielectric constant of the interlayer medium.

Theoretically, our result for $\lambda_\perp$ can be compared with various expressions which make use of the normal-state conductivity, assuming either specular or diffuse interlayer pair transfer. For specular transfer (momentum conserved parallel to the planes), the interlayer Josephson current density is given for $T \ll T_c$ by $J_0 = 2eN_0\tau_\perp^2/\hbar$, where N_0 is the single-particle density of states at the Fermi energy, and $\tau_\perp$ is the interlayer hopping time [21]. The normal-state interlayer conductance, given the same assumptions, is $\sigma_\perp = 4e^2 s N_0 \tau_\perp^2 \tau/\hbar^2$, with $\tau^{-1} = \tau_\parallel^{-1} + 2\tau_\perp^{-1}$ [21]. Then, writing the interlayer normal-state resistivity per plane as $\rho = s/\sigma_\perp$, where s is the interlayer spacing, we have the expression $J_0 = \hbar/2\rho_\perp \tau e$. Taking the measured value at $T = 12$ K for the in-plane normal-state conductance $\sigma_\perp = 3.8 \times 10^3$ $(\Omega\ \mathrm{cm})^{-1}$ [22], estimating the anisotropy ratio to be $\sigma_\parallel/\sigma_{perp} \sim 1000$ [23], and taking τ to be in the range $2\,\mathrm{cm}^{-1} < (2\pi\tau c)^{-1} < 20\,\mathrm{cm}^{-1}$ [22], we estimate that $3\times10^3\,\mathrm{A\,cm}^{-2} < J_0 < 3\times10^4\,\mathrm{A\,cm}^{-2}$. Then equation (1) leads to the rough estimate 20 μm $< \lambda_\perp <$ 70 μm, consistent with our experimental value. For diffusive pair transfer (parallel momentum not conserved) [24–26], the Josephson current density between two identical superconducting sheets at $T = 0$ is given by $J_0 = \pi\Delta_0/2e\rho_\perp$ [27] where Δ_0 is the zero-temperature energy gap. Using the previous estimate for $\rho_\perp$ and the BCS value $\Delta_0 = 1.76\ k_B T_c$, we make the rough estimate $J_0 \sim 5 \times 10^4$ A cm^{-2}, and $\lambda_\perp < 20$ μm. Quantitative comparison with more exact measurements of $\rho_\perp$ would be quite useful, since the supercurrent can be sharply reduced relative to the normal-state conductance if there is unconventional (e.g. d-wave) pairing and diffusive interlayer transport [26]. The details of the band structure should also be considered.

In the interlayer tunnelling (ILT) model, the interlayer coupling in the superconducting state is the source of the superconductivity, and so the interlayer penetration depth is much more tightly constrained in this model than it is in the phenomenological models. Single-particle tunnelling between layers is severely reduced in the normal state in the ILT model, but interlayer pair tunnelling is allowed in the superconducting state. A reduction of the charge-carrier kinetic energy due to pair tunnelling provides the condensation energy required for the superconducting transition. Thus, if this model is correct, one naively expects a strong interlayer coupling, and therefore a short $\lambda_\perp$. In Leggett's formulation, the experimentally measured value $\lambda_\perp$ should be compared to $\lambda_{ILT} \sim 10$ μm given by equation (2) [8]. It has been argued that this model is the mechanism of the superconductivity in some organic superconductors [28, 29]. In current published versions of the theory, $\lambda_\perp$ is equal to λ_{ILT} within a factor of 2, and it has been argued that as the experimentally measured value of $\lambda_\perp$ becomes larger, the model becomes less plausible [7, 8].

Combining our value for the interplane penetration depth of $\sim$60 μm with a value for the in-plane penetration depth of $\sim$0.5 μm [19], we obtain a superconducting anisotropy ratio

of about 100, slightly smaller than estimated previously but still putting this material in the regime of the highly anisotropic superconductors. This has profound consequences for the low-field phase diagram of the vortices, since it influences the stiffness of the pancake vortex stack. Thus our results provide important information for understanding the vortices in this material.

In previous magnetic images of vortices, the spatial resolution of the sensor has been comparable to, or perhaps a few times larger than, the penetration depth [30–34]. The images shown here are the first quantitative magnetic images to have a spatial resolution much smaller than the size of the vortex. This method provides a direct measure of the interlayer coupling strength. The shape of the interlayer vortices in this layered superconductor agrees well with the Kogan–Clem model [3], which is based on the usual assumption of weakly coupled superconducting layers.

Acknowledgments

We thank P M Chaikin for numerous useful discussions beginning with the inception of this experiment. We also thank D J Scalapino for assistance with the theoretical length estimates, P W Anderson and S Chakravarty for useful discussions, and M B Ketchen, M Bhushan, and A Ellis for technical assistance. K A Moler would like to acknowledge the support of an R H Dicke Postdoctoral Fellowship, and NSF funding through the MRSEC award to Princeton University (DMR 97-00362). The work at Argonne was sponsored by the Department of Energy, Office of Basic Energy Sciences, Division of Materials Sciences, under Contract W-31-139-ENG-38.

References

[1] Lawrence W E and Doniach S 1971 *Proc. 12th Int. Conf. on Low Temperature Physics* ed E Kanda (Kyoto: Academic) p 361
[2] Clem J R and Coffey M W 1990 *Phys. Rev.* B **42** 6209
Clem J R, Coffey M W and Haro Z 1991 *Phys. Rev.* B **44** 2732
Gurevich A, Benkraouda M and Clem J R 1996 *Phys. Rev.* B **54** 13 196
[3] Kirtley J R, Kogan V G, Clem J R and Moler K A 1999 *Phys. Rev.* B at press
[4] Wheatley J, Hsu T and Anderson P W 1968 *Nature* **333** 121
[5] Anderson P W 1991 *Physica* C **185** 11
Anderson P W 1991 *Phys. Rev. Lett.* **67** 660
Anderson P W 1992 *Science* **256** 1526
[6] Chakravarty S, Sudbø A, Anderson P W and Strong S 1993 *Science* **261** 331
[7] Anderson P W 1995 *Science* **268** 1154
[8] Leggett A J 1996 *Science* **274** 587
[9] Mansky P A, Chaikin P M and Hadden R C 1994 *Phys. Rev.* B **50** 15 929
[10] Schlenga K *et al* 1994 *Physica* C **235–240** 3273
[11] Shibauchi T, Sato M, Mashio A, Tamegai T, Mori H, Tajima S and Tanaka S 1997 *Phys. Rev.* B **55** R11 977
[12] Tsvetkov A A *et al* 1998 *Nature* **395** 360
[13] See, for example, the summary in
Lang M, Toyota N and Sasaki T 1993 *Synth. Met.* **55–57** 2401
[14] Kanoda K, Akiba K, Suzuki K, Takahashi T and Saito G 1990 *Phys. Rev. Lett.* **65** 1271
[15] Takahashi T, Kanoda K and Saito G 1991 *Physica* C **185–189** 366
[16] Kanoda K, Kawamoto A, Oshima K, Takahashi T, Kikuchi K, Saito K and Ikemoto I 1993 *Synth. Met.* **56** 2865
[17] Klein O, Holczer K, Grüner G, Chang J J and Wudl F 1991 *Phys. Rev. Lett.* **66** 655
[18] Kirtley J R, Ketchen M B, Stawiasz K G, Sun J Z, Gallagher W J, Blanton S H and Wind S J 1995 *Appl. Phys. Lett.* **66** 1138
[19] Lee S L *et al* 1997 *Phys. Rev. Lett.* **79** 1563
[20] Carlson K D *et al* 1988 *Inorg. Chem.* **27** 965

[21] Bulaevski L N 1973 *Sov. Phys.–JETP* **37** 1133
[22] Dressel M, Bruder S, Grüner G, Carlson K D, Wang H H and Williams J M 1993 *Phys. Rev.* B **48** 9906
[23] Oshima K, Urayama H, Yamochi H and Saito G 1988 *Physica C* **153–155** 1148
[24] Graf M J, Rainer D and Sauls J A 1993 *Phys. Rev.* B **47** 12 089
[25] Rojo A G and Levin K 1993 *Phys. Rev.* B **48** 16 861
[26] Hirschfeld P J, Quinlan S M and Scalapino D J 1997 *Phys. Rev.* B **55** 12 742
[27] Ambegaokar V and Baratoff A 1963 *Phys. Rev. Lett.* **10** 486
Ambegaokar V and Baratoff A 1963 *Phys. Rev. Lett.* **11** 104 (erratum)
[28] Clarke D G, Strong S P, Chaikin P M and Chashechkina 1998 *Science* **279** 2071
[29] Baskaran G 1997 *Phil. Mag.* B **71** 119
[30] Chang A M *et al* 1992 *Appl. Phys. Lett.* **61** 1974
Chang A M, Hallen H D, Hess H F, Kao H L, Kwo J, Sudbo A and Chang T Y 1992 *Europhys. Lett.* **20** 645
[31] Moser A, Hug H J, Parashikov I, Stiefel B, Fritz O, Thomas H, Baratoff A, Güntherodt H-J and Chaudhari D 1995 *Phys. Rev. Lett.* **74** 1847
[32] Kirtley J R, Tsuei C C, Rupp M, Sun J Z, Yu-Jahnes L S, Gupta A, Ketchen M B, Moler K A and Bhushan M 1996 *Phys. Rev. Lett.* **76** 1336
[33] Moler K A, Kirtley J R, Hinks D G, Li T W and Xu M 1998 *Science* **279** 1193
[34] Kirtley J R, Moler K A, Villard G and Maignan A 1998 *Phys. Rev. Lett.* **81** 2140